PROCEEDINGS OF THE INTERNATIONAL CONFERENCE NANOMATERIALS: APPLICATIONS AND PROPERTIES
Vol. **3** No 1, 01NTF01(3pp) (2014)

Two-dimensional Electron-hole Liquid in Systems of Spatially Direct and Indirect Excitons in Si / SiGe Heterostructures

T.M. Burbaev *, D.S. Kozyrev, N.N. Sibeldin, M.L. Skorikov

Lebedev Physical Institute of the Russian Academy of Sciences, 53, Leninskii Pr., 119991 Moscow, Russia

(Received 11 March 2014; published online 29 August 2014)

The two-dimensional electron-hole liquid (EHL) in 2- and 4-nm-thick SiGe layers of $Si/Si_{0.91}Ge_{0.09}/Si$ heterostructures is discovered and its properties are studied by photoluminescence (PL) spectroscopy in the near-infrared and visible spectral ranges at low temperatures. It is shown that the PL in the visible range observed at high excitation levels originates from two-electron recombination transitions in the EHL. For the SiGe layer thickness $d = 2$ nm, the barrier formed by this layer for electrons in the conduction band is tunnel-transparent, and the EHL is spatially direct. For $d = 4$ nm, this barrier is nontransparent, and the EHL has dipolar character, with holes being confined in the SiGe layer and electrons occupying Si layers. It is found that the binding energy and the critical temperature of the dipolar EHL is substantially less than the spatially direct.

The binding energy of free biexcitons in the tunnel-transparent SiGe layer is determined.

Keywords: Electron-hole liquid, Biexciton, Quasi-two-dimensional layers, Heterostructures, Photoluminescence.

PACS numbers: 73.20.Mf, 78.67.De

1. INTRODUCTION

It is well known that, at low temperatures, the ground state of a nonequilibrium electron-hole system with sufficiently high density in bulk silicon and germanium corresponds to metallic electron-hole liquid (EHL), into which excitons condense [1-5]. In bulk materials, the spatial distribution of nonequilibrium electrons and holes coincide. In contrast, in type-II $Si / Si_{1-x}Ge_x / Si$ heterostructures, systems where electrons and holes are spatially separated can be prepared. In these structures, a strained $Si_{1-x}Ge_x$ layer clad between thick Si layers forms a deep potential well for holes in the valence band and a relatively low barrier for electrons in the conduction band. Electrons, which are attracted to quantum-confined holes, can also penetrate into the barrier. Varying the thickness d of the SiGe layer, one can obtain systems with either spatially direct excitons (for small d) or spatially indirect (dipolar) excitons (Fig. 1). Here, we investigated multiparticle excitations in such systems using the spectroscopy of photoluminescence (PL) in the near-infrared (NIR) and visible spectral ranges.

2. EXPERIMENTAL

Strained-layer SiGe structures were grown by molecular-beam epitaxy on Si (001) substrates. Thicknesses of the buffer and the cap Si layers were 100 nm and 100-200 nm, respectively. The PL spectra in the NIR spectral range were recorded for the sample temperatures $T = 2$–60 K and excitation levels $P = 0.05$-300 W/cm². A He-Cd laser was used as the PL excitation source and the recombination radiation was analyzed by a grating monochromator and detected by a liquid-nitrogen-cooled Ge p–i–n photodiode.

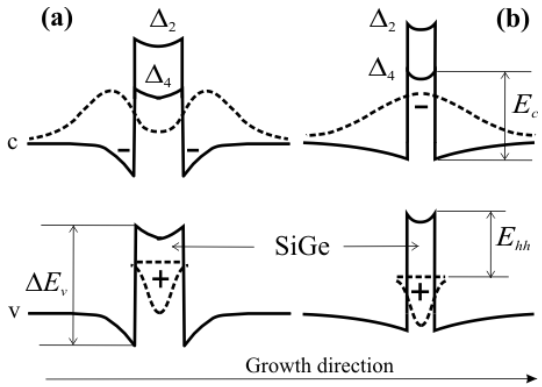

Fig. 1 – Schematic band diagrams of $Si/Si_{1-x}Ge_x/Si$ heterostructures with the SiGe layer thickness $d = 4$ (a) and (b) 2 nm. Dashed lines show the electron-density distribution along the growth axis and the heavy-hole quantum-confinement level for each structure

Also, spectra of the PL in the visible range were recorded. This PL results from the so-called two-electron transitions, i.e., from simultaneous recombination of two electrons and two holes accompanied by the emission of a single photon whose energy equals the total energy of the four recombining particles [6, 7]. These measurements were carried out for $T = 15$ K and $P = 0.3$-150 W/cm². A Ti-sapphire laser tuned to $\lambda = 0.75$ μm was used as the PL excitation source. The recombination radiation was analyzed by a grating spectrometer and detected by a liquid-nitrogen-cooled CCD matrix. A comparison of one- and two-electron spectra makes for more reliable identification of different components in the conventional (one-electron) PL spectra, since lines in the two-electron spectra cannot originate from species containing less than two electron-hole pairs.

* burbaev@sci.lebedev.ru

3. RESULTS AND DISCUSSION

Figure 2 presents the NIR PL spectra for two structures in which the $Si_{1-x}Ge_x$ layer has the same composition ($x \approx 0.09$) but different thicknesses $d = 4$ nm (sample #4, Fig. 2a) and 2 nm (sample #2, Fig. 2b). The figure shows the most intense components of the PL, resulting from the simultaneous emission of a photon and a TO phonon. At low excitation levels (Fig. 2a, curves 1-5; Fig. 2b, curves 1-4), the exciton PL lines are observed in the short-wavelength part of the spectrum. Excitons are free at high temperatures. In structure #4, dipolar excitons are free for $T \geq 23$ K; in structure #2, spatially direct excitons are free for $T \geq 12$ K. With decreasing temperature, excitons become localized in the wells of the random lateral potential originating from the compositional inhomogeneity in the SiGe layer plane and at heterointerfaces; the exciton localization is accompanied by a red shift of the corresponding PL lines, as indicated in Fig. 2a. In addition, a decrease in the temperature brings about the appearance of the biexciton PL lines on the red side of the exciton lines. Thus, the PL of localized dipolar biexcitons is observed in structure #4, while the PL of free spatially direct biexcitons is observed in structure #2 for $T \geq 12$ K. The dependence of the biexciton PL intensity on the excitation level is linear in the first case and close to quadratic in the second case. At high excitation levels and low temperatures, the spectra are dominated by the emission from the EHL, which is spatially direct in structure #2 (Fig. 2b, curve 5) and indirect in structure #4 (Fig. 2a, curves 6, 7).

It is known that independence of the PL line shape from the excitation level is a signature of the EHL luminescence. According to Fig. 2a, the normalized shapes of the PL spectra of sample #4 recorded at $T = 1.8$ K for two pump powers differing by a factor of 2 (curves 6, 7) coincide. The shape and position of the PL lines recorded for the same pump level in the temperature range of 1.8-6 K also coincide with those of curves 6 and 7. The dipolar EHL in structure #4 is composed by heavy holes in the quantum well formed in the valence band by the SiGe layer and electrons from Δ_4 valleys of the conduction band of Si, which are bound to the holes by Coulomb attraction and occupy triangular potential wells formed at Si / SiGe heterointerfaces owing to the band bending at high excitation levels. In this case, the calculated luminescence line is described by two-dimensional density of states both for heavy holes and Δ_4 electrons (Fig. 2a, dashed line). The calculated profile of the luminescence line of spatially direct EHL in structure #2 is shown in Fig. 2b (curve 5, solid line) [1]. The difference between the EHL luminescence line shape in structures #2 and #4 originates from the difference in the energy dependences of the electron density of states ρ ($\rho \sim E^{1/2}$ for *#2* and $\rho = \text{const}$ for #4). In addition, the ratio F_e / F_h of the electron and hole Fermi energies, which affects the shape of the EHL luminescence line, is different in the two cases. Comparing the energy separation between the EHL and FE lines in Figs. 2a and 2b, one can see that the binding energy in the dipolar EHL is considerably lower than in the spatially direct EHL.

The variation of the PL spectra of structures #4 and #2 in the visible range with increasing excitation level is shown in Fig. 3. The visible-range PL originates from simultaneous recombination of two holes in the valence

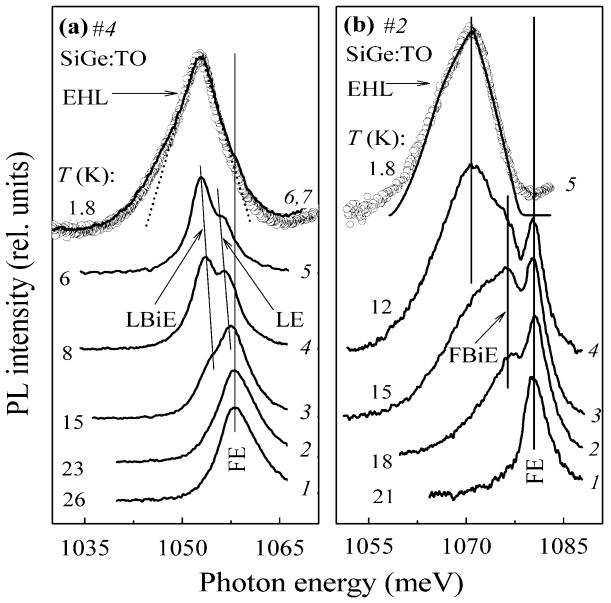

Fig. 2 – Modification of the NIR PL spectra of structures (a) #4 and (b) #2 with decreasing temperature T and increasing pump power P.
(a) Curves 1-5: T varies between 26 and 6 K, $P = 0.12$ W/cm². Curves 6 and 7 (shown overlapping by circles and solid line, respectively): $T = 1.8$ K, $P = 85$ and 170 W/cm², respectively; dashed line shows the calculated spectrum of the dipolar EHL luminescence.
(b): Curves 1-4: T varies between 21 and 12 K, $P = 2$ W/cm². Curve 5 (circles): $T = 1.8$ K, $P = 4$ W/cm²; solid line shows the calculated spectrum of the spatially direct EHL luminescence [8].
FE, FBiE, LBiE, and EHL stand for free excitons, free biexcitons, localized biexcitons, and electron-hole liquid, respectively. Normalized spectral curves are shown in all cases

band in the SiGe layer and two electrons from the opposite valleys in the conduction band. Thus, the PL resulting from these so-called two-electron transitions occurs at photon energies approximately a factor of 2 higher than the energies of no-phonon (NP) single-electron transitions in the NIR range. Narrow lines in Fig. 3 correspond to the biexciton luminescence, and wide lines, to the EHL luminescence. At low excitation levels, biexcitons in structure #4 are observed in the temperature range of 1.8-23 K. As the temperature decreases to 1.8 K, they become localized; similarly to the NIR PL spectra, this is accompanied by a red shift of the biexciton PL line. The dipolar EHL appears at higher excitation levels. The shape and position of the corresponding PL line become independent of the excitation level as the latter is raised still further and hardly depend on temperature for $T = 1.8$-6 K.

The modification of the visible-range PL spectra of structure #2 with increasing pump level at $T = 15$ K is shown in Fig. 3b. At low excitation levels, a narrow PL line of free biexcitons (FWHM ≈ 4 meV) is clearly observed. At high excitation levels, the spectra are dominated by a broad (FWHM ≈ 20 meV) PL line of the EHL. Similarly to the NIR spectra, the shape of this line ultimately becomes independent of the excitation level (compare curves 3 and 4), which is a feature characteristic of the EHL luminescence. In this case, the EHL is spatially direct, and its binding energy and critical temperature are considerably higher than those

for the dipolar EHL. At 15 K, the EHL line shape is to a large extent determined by temperature effects. At 1.8 K (curve 5, circles), the lineshape is determined only by the behavior of $\rho(E)$ and the electron and hole Fermi energies in the EHL. Here, the solid line shows the numerical convolution of the corresponding spectrum

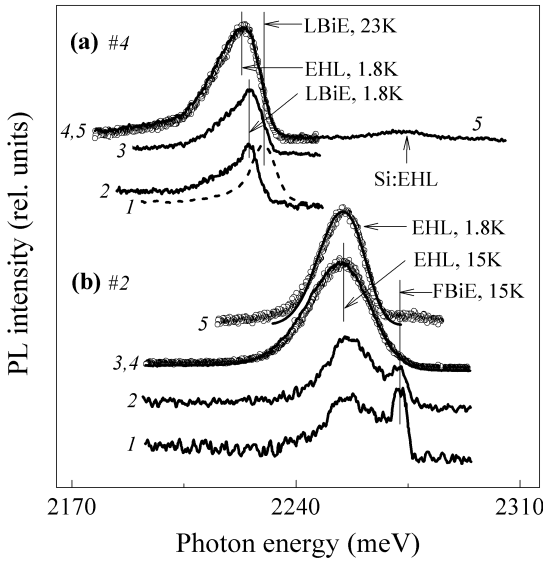

Fig. 3 – Modification of the visible-range PL spectra with increasing pump power.
(a) Structure #4. T = 1.8 K, P = (2) 3.8, (3) 13, (4) 108, and (5) 180 W/cm²; curves 4 (circles) and 5 (solid line) are shown overlapping. Curve 1 (dashed line) shows the biexciton PL spectrum observed for T = 23 K and P = 3.5 W/cm².
(b) Structure #2. T = 15 K, P = (1) 0.5, (2) 1.0, (3) 85, and (4) 150 W/cm²; curves 3 (circles) and 4 (solid line) are shown overlapping. Curve 5 (dashed line) shows the PL spectrum recorded for T = 1.8 K and P = 260 W/cm²; the solid line shows the numerical convolution of the experimental spectrum 5 (Fig. 2b).
Normalized spectral curves are shown in all cases

recorded in the NIR range (Fig. 2b, curve 5). Good agreement between the experimentally determined shape of the visible PL line and the convolution of the EHL luminescence line recorded in the NIR range indicates that the nature of the PL lines in the two cases is the same. Thus, we observe the single-electron and two-electron recombination radiation of the spatially direct quasi-two-dimensional EHL in the NIR and visible PL spectra, respectively.

Combining data from the NIR and visible PL spectra, one can determine the binding energy of free biexcitons E_M:

$$E_M = 2[h\nu_{NIR}(\text{FE-NP})] - h\nu_{VIS}(\text{FBiE}),$$

where $h\nu_{NIR}$ and $h\nu_{VIS}$ are photon energies of the NIR and visible PL corresponding to the excited states indicated in parentheses. It is convenient to reference all energies to the EHL luminescence energy and to use intense TO-phonon components of the NIR spectrum as follows:

$$E_M = 2[h\nu_{NIR}(\text{FE-TO}) - h\nu_{NIR}(\text{EHL-TO})] - [h\nu_{VIS}(\text{FBiE}) - h\nu_{VIS}(\text{EHL})].$$

Taking the required photon energies from the spectra in Figs. 2 and 3, we obtain $E_M = 2.0 \pm 0.5$ meV. The value of the binding energy of quasi-two-dimensional free biexcitons thus obtained exceeds noticeably the free-biexciton binding energy in the three-dimensional case (in bulk uniaxiallystrained Si, $E_M \approx 1.3$-1.4 meV [9]).

AKNOWLEDGEMENTS

We are grateful to L.V. Keldysh and A.P. Silin for interest in this study and useful discussions; D.V. Shepel' and V.A. Tsvetkov for help with experimental work; D.N. Lobanov and A.V. Novikov for growing the Si / SiGe heterostructures.

This study was supported by the Russian Foundation for Basic Research (projects nos. 13-02-00853, 13-02-904 67), and Programs of fundamental studies of the Russian Academy of Sciences.

REFERENCES

1. L.V. Keldysh, *Proceedings of 9th International Conference on the Physics of Semiconductors, Moscow, 1968* (Leningrad: Nauka: 1969).
2. T.M. Rice, J.C. Hensel, T.G. Fillips, G.A. Thomas, *Solid State Physics* **32**, (New York: Academic Press: 1977).
3. *The Electron-Hole Drops in Semiconductors, in: Modern Problems in Condensed Matter Sciences*, **6**, (Eds. by C.D. Jeffries, L.V. Keldysh), (Amsterdam: North-Holland: 1983).
4. L.V. Keldysh, N.N. Sibeldin, *Ibid*, **16**, (Eds. by W. Eisenmenger, A.A. Kaplyanskii) (1986).
5. N.N. Sibeldin. *Electron-Hole Liquid in Semiconductors, in: Problems of Condensed Matter Physics: Quantum Coherence Phenomena in Electron-Hole and Coupled Matter-Light System*, (Eds. by A.L. Ivanov, S.G. Tikhodeev), *International Series of Monographs on Physics* **139**, p.227, (Oxford University Press: 2008).
6. K. Betzler, R. Conradt, *Phys. Rev. Lett.* **28**, 1562 (1972).
7. T.W. Steiner, L.C. Lenchyshyn, M.L.W. Thewalt, J.P. Noel, N.L. Rowell, D.C. Houghton, *Solid State Commun.* **89**, 429 (1994).
8. D. Shepel, T. Burbaev, N. Sibeldin, M. Skorikov, *phys. status solidi c* **8**, 1186 (2011).
9. V.D. Kulakovskii, V.G. Lysenko, V.B. Timofeev, *Sov. Phys. Usp.* **28**, 735 (1985).